CHEMISTRY
A EUROPEAN JOURNAL

Structure and Bonding of Zinc Antimonides: Complex Frameworks and Narrow Band Gaps

Arkady S. Mikhaylushkin, Johanna Nylén, and Ulrich Häussermann*[a]

Abstract: We investigated crystal structure relationships, phase stability and chemical bonding of the thermoelectric materials ZnSb, α-Zn_4Sb_3, and β-Zn_4Sb_3 by means of first principles calculations. The structures of these materials are difficult to rationalise. This is especially true for β-Zn_4Sb_3 because of the presence of vacancies and interstitial atoms. We recognised rhomboid rings Zn_2Sb_2 as central structural building units present in all materials. Importantly, these rings enable to establish a clear relationship between disordered β-Zn_4Sb_3 and ordered low-temperature α-Zn_4Sb_3. Concerning the phase stability of Zn_4Sb_3 we identified a peculiar situation: α-Zn_4Sb_3 is metastable and β-Zn_4Sb_3 can only be thermodynamically stable when its structural disorder accounts for a large entropy contribution to free energy. According to their electronic structure zinc antimonides represent heteroatomic framework structures with a modest polarity. The peculiar electronic structure of Zn/Sb systems can also be modelled by Al/Si systems. The high coordination numbers in the frameworks implies the presence of multicentre bonding. We developed a simple bonding picture for these frameworks where multicentre bonding is confined to rhomboid rings Zn_2Sb_2.

Keywords: antimony · intermetallic phases · polymorphism · semiconductors · zinc

Introduction

Probing solid-state materials at the boundary between metals and nonmetals is an exciting field of research. The intermediate region between valence compounds and fully delocalised metallic systems exhibits a rich, unique, structural chemistry and interesting physical properties.[1–3] The peculiarity of the metal–nonmetal border is splendidly exemplified by binary zinc antimonides, which combine remarkable thermoelectric figures of merit with an immense structural complexity. The Zn/Sb system affords three fields of phases which are located in the narrow range between 50 and 60 atom % Zn.[4,5] ZnSb is a stoichiometric compound with a well characterised crystal structure (CdSb-type)[6] and stable up to 822 K. Zn_4Sb_3 displays involved temperature polymorphism.[7–10] At around 250 K the transition α → β takes place. β-Zn_4Sb_3 is succeeded by γ-Zn_4Sb_3 above approximately 765 K. At even higher temperatures two more modifications are proposed (δ and δ′).[5] Zn_3Sb_2 is metastable and appears in a low-temperature (between 677 and 714 K) and high-temperature form (between 677 and 841 K). The structures and exact compositions of the Zn_4Sb_3 and Zn_3Sb_2 phases have been either reported controversially or fragmentary. Only very recently β-Zn_4Sb_3 was recognised as substantially disordered[11,12] and the structure of high-temperature Zn_3Sb_2 could be identified as a complex incommensurately modulated one with the modulation vector coupled to a small homogeneity range $Zn_{3-x}Sb_2$ ($0.167 < \times < 0$).[13]

ZnSb and Zn_4Sb_3 are narrow gap semiconductors and have interesting thermoelectric properties.[14,15] (The properties of Zn_3Sb_2 are virtually unknown.) In particular, β-Zn_4Sb_3 is considered to be a state-of-the-art material at moderate temperatures (450–650 K) closing the gap between low-temperature materials (Bi_2Te_3 based systems) and intermediate temperature materials ($AgSbTe_2$–GeTe based systems (TAGS)).[16] A good thermoelectric material requires that a high thermopower S is combined with a low electrical resistivity ρ and a low thermal conductivity κ.[17] Interestingly, the values and temperature behaviour for S and ρ are very similar for ZnSb and β-Zn_4Sb_3. What makes β-Zn_4Sb_3 special is the exceptional thermal conductivity, which is as low as that for glass-like materials.[16] The discovery of disordered Zn in β-Zn_4Sb_3 provides a plausible reason for this phenomenon and stresses an important issue: Prior to understanding the complex interplay of different transport properties defining thermoelectric efficiency, very careful

[a] Dr. A. S. Mikhaylushkin, J. Nylén, Dr. U. Häussermann
Inorganic Chemistry, Stockholm University
10691 Stockholm (Sweden)
Fax: (+46) 8-152-187
E-mail: ulrich@inorg.su.se

DOI: 10.1002/chem.200500020

crystallographic studies of the considered material have to be performed, in order to unambiguously determine its structure and composition.[12,18,19]

Recently we reported on the complex structure of low-temperature α-Zn_4Sb_3.[20] Surprisingly, this phase is completely ordered and, furthermore, the order-disorder α–β transition occurs reversibly in single crystal X-ray diffraction experiments. We could show that the crystallographic composition of α-Zn_4Sb_3 is $Zn_{13}Sb_{10}$ ($Zn_{3.9}Sb_3$), which implies that the actual composition of disordered β-Zn_4Sb_3 has to be $Zn_{13}Sb_{10}$ as well. As a matter of fact, only a composition $Zn_{13}Sb_{10}$ is compatible with the narrow gap semiconductor properties of both forms of Zn_4Sb_3. In this work we present a clear relationship between the crystal structures of α- and β-Zn_4Sb_3. Additionally we perform a detailed analysis of the electronic structure and phase stability of ZnSb and Zn_4Sb_3 by means of first principles calculations. Finally we attempt to rationalise the bonding properties of the complex ZnSb and Zn_4Sb_3 framework structures by a simple model, which accounts for the narrow band gap. Our study aims at a deeper understanding of the complex phase and structural relations, and eventually also the origin of properties, in the remarkable Zn/Sb materials. Such an understanding is of utmost importance for possibly optimising the thermoelectric performance of these materials by, for example, controlled doping.

Structural Relationships

ZnSb: The structure of orthorhombic ZnSb (space group *Pbca*, $Z = 8$) was reported already in 1948.[6] Zn and Sb both occupy general positions and attain a peculiar five-fold coordination by one like and four unlike neighbours (Figure 1a). The nearest neighbour distances vary between 2.67 and 2.84 Å and are well separated from the next nearest ones starting off at 3.66 Å. ZnSb may be regarded as an arrangement of Zn centred, vertex and corner sharing, Sb_4 tetrahedra (quasitetrahedral close-packing). However, we prefer to focus on the planar rhomboid rings Zn_2Sb_2 (diamonds) containing the Zn–Zn contact as central building units. In ZnSb each diamond is linked to 10 neighbouring ones. Figure 1b shows a layer of diamonds in the *ac* plane. In such a layer each diamond is surrounded by six neighbouring ones, two are attached to the Sb atoms and one to the Zn atoms. This leaves one coordination site per atom to bind diamonds in the *b* direction (two up and two down, Figure 1c). (Note, that because of the three axial glides this description holds for any direction.)

Zn_4Sb_3: Zn_4Sb_3 occurs in at least three modifications.[5] The crystal structures of α- and β-Zn_4Sb_3 could be characterised properly only recently, the structures of the high-temperature polymorph(s) still await solution.[11,12,20] The structure of β-Zn_4Sb_3 is rhombohedral (space group $R\bar{3}c$) and contains three distinct atomic positions (36 Zn, 18 Sb1, and 12 Sb2). The structure of α-Zn_4Sb_3 is triclinic, conveniently described

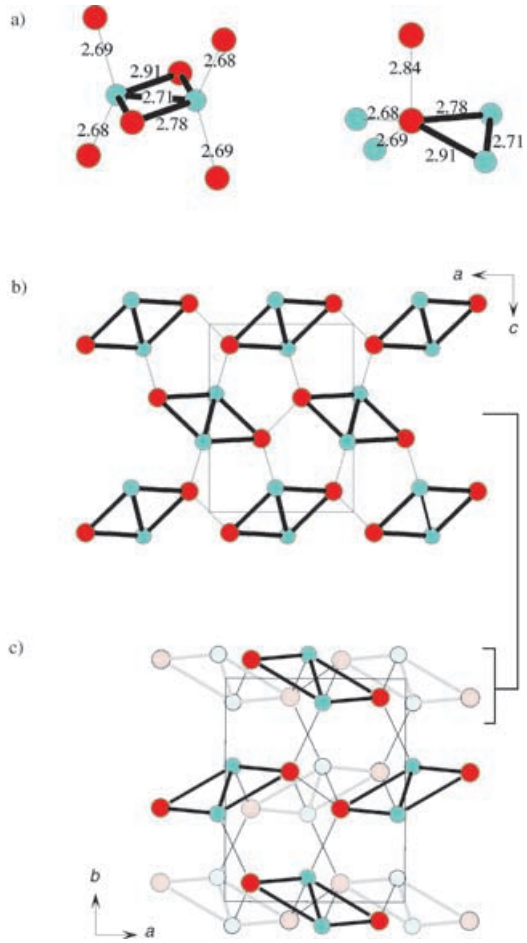

Figure 1. Crystal structure of orthorhombic ZnSb: Zn (●) and Sb (●) atoms, respectively. The rhomboid (diamond) ring Zn_2Sb_2 is used as central structural building unit and emphasised by bold lines, the remaining nearest neighbour contacts are drawn as thin lines. a) Coordination environment for Zn (right) and Sb (left). The inserted numbers indicate interatomic distances in Å. b) A layer of diamonds in the *ac* plane. c) Two layers of diamonds along the *c* direction related by glide operation. The layers are distinguished by dark and pale colour.

with a C-centred, *metrically monoclinic* cell (space group $C\bar{1}$), and contains 26 Zn and 20 Sb general positions. Both structures are composed of Zn_2Sb_2 diamonds, that is, the structural unit already identified in the ZnSb structure (Figure 2a). As a matter of fact, the coordination of Zn atoms in α and β-Zn_4Sb_3 appears to be identical to that in ZnSb. However, in β-Zn_4Sb_3 diamonds form chains by sharing common Sb1 atoms. These chains run in three different directions in the rhombohedral structure and result in a framework with channels along the *c* direction (Figure 2b). The channels are centred by Sb2 atoms, which are located on the three-fold axes. Sb2 atoms display alternating short (2.82 Å) and long (3.39 Å) contacts to each other. Additionally, each Sb2 atom is coordinated to three Zn atoms within diamonds and thus attains a tetrahedral environment (Figure 2a). Sb1 atoms are exclusively surrounded by Zn atoms (six, at distances between 2.7 and 2.8 Å). Four of these Zn atoms are located within the same diamond chain and two in neighbouring chains.

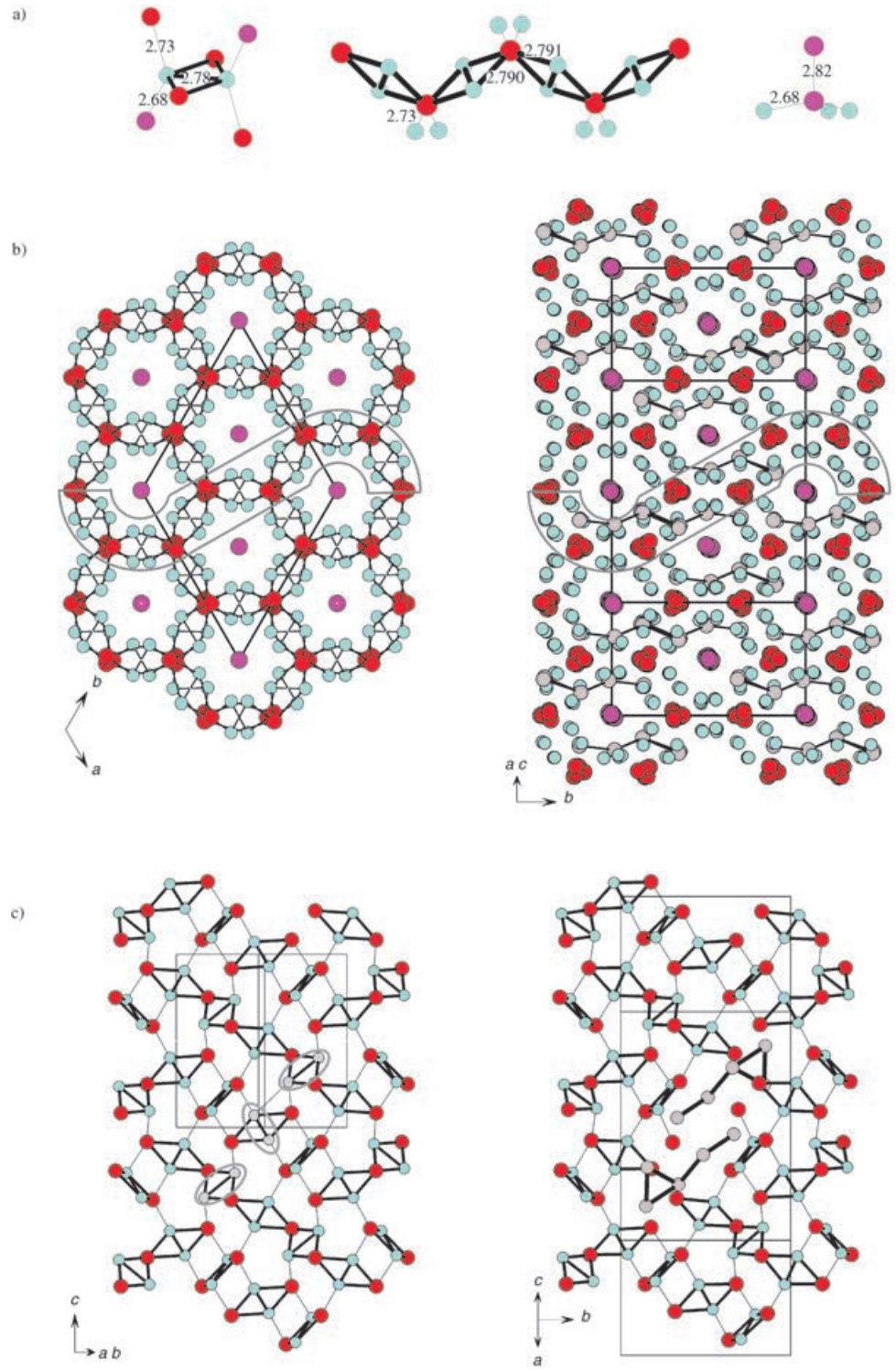

Figure 2. Comparison of the crystal structures of triclinic α-Zn_4Sb_3 and rhombohedral β-Zn_4Sb_3. Note that the unit cell of α-Zn_4Sb_3 is monoclinic C-centred: Zn atoms (●), two different types of Sb atoms: Sb1 (●) and Sb2 (●). The rhomboid (diamond) ring Zn_2Sb_2 is used as central structural building unit and emphasised with bold lines. a) Coordination environment for Zn (right), Sb1 (middle), and Sb2 (left). The inserted numbers indicate interatomic distances in Å found in the idealised rhombohedral framework of β-Zn_4Sb_3. b) Left: Idealised framework (Zn_6Sb_5) of β-Zn_4Sb_3 along [001]. The framework is built from chains of condensed diamonds $Zn_2Sb1_{2/2}$ (cf. Figure 2a, middle) and consists of channels, which are stuffed by Sb2 atoms. Right: Structure of α-Zn_4Sb_3 along [30$\bar{1}$] which is equivalent to the [001] direction in β-Zn_4Sb_3. Grey circles denote "non-rhombohedral" Zn atoms, that is, Zn atoms with no counterpart in Zn_6Sb_5. Distances below 3 Å between "non-rhombohedral" Zn atoms are drawn as lines in order to emphasise the location of these atoms. Lines defining diamond rings are not drawn for clarity. c) Left: Section of the $Zn_2Sb1_{2/2}$ framework of β-Zn_4Sb_3 (marked in Figure 2b) rotated by 90° (yielding approximately the [1$\bar{1}$0] direction). Sb2 atoms are not shown for clarity. Grey circles highlight pairs of Zn atoms present in Zn_6Sb_5 but absent in α-Zn_4Sb_3. Right: Equivalent section of the α-Zn_4Sb_3 structure. Two five-atom clusters of non-rhombohedral Zn atoms ("interstitials") replace three pairs of Zn atoms from the rhombohedral framework ("vacancies").

The unit cell content of the above-described rhombohedral framework of β-Zn_4Sb_3 amounts to just $Zn_{36}Sb_{30}$ ($Zn_{3.6}Sb_3$). The deviation from the nominal (i.e., synthesis) composition[21] and its implication to crystal structure has been the subject of controversy.[10,22] A detailed solution to the problem was finally obtained by Snyder et al. and Cargoni et al. when identifying a high degree of disorder in the Zn substructure of β-Zn_4Sb_3.[11,12] By analysing the experimental electron density, which was calculated by the maximum entropy method from high-resolution synchrotron powder diffraction data, they found interstitial Zn atoms distributed on three weakly occupied general sites in space group $R\bar{3}c$ (36f). Additionally, the regular framework position (also 36f) of the pairs of Zn atoms within the diamonds displayed a considerable occupational deficiency (0.89–0.9). The composition obtained from the refined occupancies of the different Zn sites is $Zn_{3.83}Sb_3$, which puts the crystallographic composition closer to the nominal one and especially removes the discrepancy between the measured and crystallographic density of β-Zn_4Sb_3.

Below about 250 K β-Zn_4Sb_3 transforms into α-Zn_4Sb_3, which somewhat surprisingly, has a completely ordered structure.[20] The C-centred unit cell of α-Zn_4Sb_3 contains 104 Zn and 80 Sb atoms and thus the composition is $Zn_{13}Sb_{10}$ ($Zn_{3.9}Sb_3$). Since the α–β transition is reversible in a single-crystal X-ray diffraction experiment the actual composition of disordered β-Zn_4Sb_3 has to be the same, for example, $Zn_{3.9}Sb_3$, which is very close to the reported values in references [11] and [12]. Figure 2b displays the structure of α-Zn_4Sb_3 along $[30\bar{1}]$ which corresponds to the *c* direction in rhombohedral β-Zn_4Sb_3. As already pointed out in our earlier work, the Sb atom substructures of α and β-Zn_4Sb_3 differ only fractionally.[20] The 80 Sb atoms (20 sites) in the unit cell of α-Zn_4Sb_3 divide into 48 atoms (12 sites) and 32 atoms (8 sites) corresponding to the Sb1 and Sb2 atoms in β-Zn_4Sb_3, respectively. A careful inspection reveals that also large parts of the Zn atom substructure are virtually identical in both structures. In Figure 2c equivalent sections of the diamond-chain framework shown perpendicular to the channel direction are compared for β- and α-Zn_4Sb_3. We note the stunning similarity, but especially the usefulness of the structural description in terms of Zn_2Sb_2 diamonds becomes apparent. This description can easily identify Zn atoms not participating in the regular framework, that is, "non-rhombohedral" Zn atoms (denoted as grey circles in Figure 2b and c). These atoms (Zn10, Zn23, Zn24, Zn25, Zn26 in the CIF[23]) are assembled in clusters consisting of a triangle with a tail of two more Zn atoms attached. Interatomic distances within this five-atom arrangement are between 2.65 and 2.93 Å. Two five-atom clusters are grouped together and related by a centre of inversion (the closest intercluster distance is around 4 Å). Each pair of five-atom clusters replaces three pairs of Zn atoms from the regular diamond-chain framework (as indicated in Figure 2c).

There are 20 "non-rhombohedral" Zn atoms (4 five-atom clusters) and 84 regular framework Zn atoms in the unit cell of α-Zn_4Sb_3. The monoclinic C-centred cell of triclinic α-Zn_4Sb_3 is by a factor $^8/_3$ larger than the hexagonal cell of rhombohedral β-Zn_4Sb_3 (note, $^8/_3$ is the ratio of Sb atoms in the two cells). When applying the situation in α-Zn_4Sb_3 to disordered β-Zn_4Sb_3 the hexagonal unit cell of the latter would contain an average of 31.5 framework Zn atoms (which are described by the regular 36f Zn position) and an average of 7.5 "non-rhombohedral" Zn atoms. It is very tempting to relate the former value to Zn vacancies present in the diamond-chain framework of β-Zn_4Sb_3 and the latter to interstitial Zn atoms. Indeed, the ratio 31.5/36 = 0.875 is close to the refined occupation of the regular Zn position in β-Zn_4Sb_3 (0.89–0.9) and the refined occupations of the interstitial positions in β-Zn_4Sb_3 sum up to about 6.5, which compares well to 7.5. To relate α- and β-Zn_4Sb_3 in this way allows a quantification of the disorder (vacancies and interstitials) in β-Zn_4Sb_3 and implies that the vacancies in the Zn framework are also present in α-Zn_4Sb_3, but occur, as the interstitial Zn atoms, completely ordered. Adding the number of vacancies (4.5) and interstitials (7.5) in the hexagonal unit cell of β-Zn_4Sb_3 amounts to a high degree of disorder ($^{12}/_{39}$, that is, about 30%) in the Zn substructure of this compound. This fact is indeed a ready explanation for its extraordinarily low, glass-like, thermal conductivity because structural disorder has a strong scattering effect to heat-carrying phonons.

In the next step we analyse the electronic structure of the ZnSb and Zn_4Sb_3 materials. Their transport properties imply that they are narrow-gap semiconductors.[24] Further, the similar electronegativity of Zn and Sb suggests that zinc antimonides are moderately polar compounds. As a matter of fact, weak polarity is a prerequisite of a good thermoelectric material because polar phonon scattering would significantly limit the mobility of electrons.[25] Thus, we expect the peculiar situation of electron precise frameworks with high coordination numbers displaying localised multi-centre bonding.

Electronic Structures

We computed the electronic density of states (DOS) of orthorhombic ZnSb, of the idealised rhombohedral framework of β-Zn_4Sb_3 with composition Zn_6Sb_5 (i.e., assuming fully occupied regular Zn position and no interstitials), and of triclinic α-Zn_4Sb_3 ($Zn_{13}Sb_{10}$) in their respective theoretical equilibrium structures. The result is assembled in Figure 3. For ZnSb (Figure 3a) the DOS is divided into distinct parts. At low energies we recognise the Sb-s band for which the bonding and antibonding component is split, and the Zn-d band. These bands have a low dispersion and are clearly detached from the succeeding valence band. The valence band is composed of Zn-s, Zn-p, and Sb-p states (Zn-d has a minor contribution) and is separated from the conduction band by a small band gap of about 0.2 eV. We note that the contribution of Zn based states to the valence band is substantial, which is anticipated from the small electronegativity difference between Zn and Sb. ZnSb can be considered as a polarised but covalently bonded framework structure. The

DOS of Zn_6Sb_5 and $Zn_{13}Sb_{10}$ are very similar to that of ZnSb (Figure 3b). For Zn_6Sb_5 the narrow band gap is above the Fermi level and a considerable amount of the valence band remains unoccupied. If existing, the material would be a good metallic conductor. Disordered β-Zn_4Sb_3, however, displays transport properties corresponding to a narrow-gap semiconductor and accordingly should have a filled valence band. Complete band filling is achieved for $Zn_{13}Sb_{10}$ (α-Zn_4Sb_3). The narrow band gap has a size of about 0.3 eV.

We now turn to the question of phase stability of ZnSb, Zn_6Sb_5, and $Zn_{13}Sb_{10}$. For that we calculated energies of formation (formation enthalpies at 0 K) with respect to elemental Zn and Sb. These energies are displayed in Figure 4. ZnSb is the most stable system with a formation energy of about 0.04 eV atom^{-1} (7.75 kJ mol^{-1} ZnSb). As expected, the non-existing idealised rhombohedral framework of β-Zn_4Sb_3 is least stable but still has a negative energy of formation. Surprising is the fact that existing α-Zn_4Sb_3 is unstable with respect to a decomposition into ZnSb and Zn. Actually its formation energy should be larger by at least 0.02 eV atom^{-1} in order to achieve a negative reaction energy for 10 ZnSb + 3 Zn = $Zn_{13}Sb_{10}$. Against this background, disorder in β-Zn_4Sb_3 has not only interesting consequences for the physical properties of this compound but has also a dramatic effect on its phase stability: Thermodynamic stability of β-Zn_4Sb_3 has to be ensured by a large entropy contribution to the free energy arising from the presence of a high degree of structural disorder. α-Zn_4Sb_3 is metastable; its decomposition into ZnSb and Zn is kinetically prevented because of the low temperature at which the α–β transition occurs.

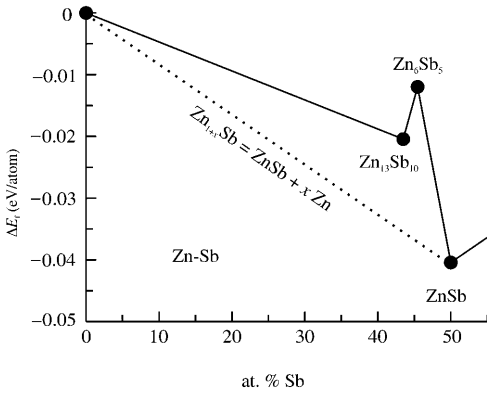

Figure 4. Energy of formation for ZnSb, Zn_6Sb_5 and $Zn_{13}Sb_{10}$. The dotted line indicates zero energy for the reaction ZnSb + xZn = $Zn_{1+x}Sb$.

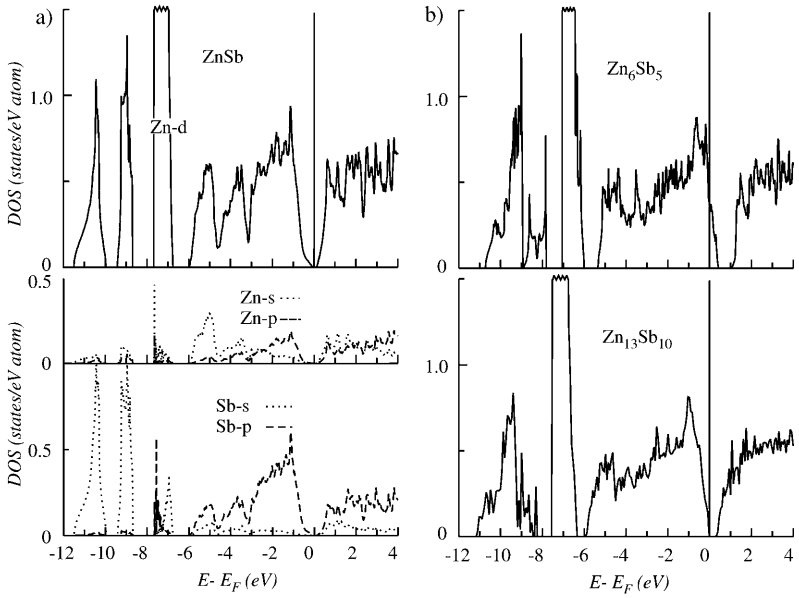

Figure 3. a) Electronic density of states (DOS) for ZnSb. Top: total DOS, bottom: site and orbital decomposed DOS. The Zn-d decomposed DOS is not shown explicitly. These states are well localised in the narrow band located around −7 eV below the Fermi level. b) DOS for Zn_6Sb_5 and $Zn_{13}Sb_{10}$. The distribution of the site and orbital decomposed components is very similar to ZnSb and not shown. The Fermi level is indicated by a vertical line.

It is interesting to investigate if the peculiar electronic structure of the zinc antimonide frameworks can also be achieved with other systems. In principle, mixtures of elements 13 and 14 may result in isoelectronic arrangements. Figure 5 shows the DOS of Al/Si systems in the structures of ZnSb, Zn_6Sb_5, and $Zn_{13}Sb_{10}$ at their respective calculated equilibrium volumes. AlSi is isoelectronic to ZnSb and indeed its DOS is very similar to that of ZnSb (compare Figure 3a). However, there are two notable differences: For AlSi the low lying, split, s band (stemming from more electronegative Si) is attached to the valence band and secondly, no real band gap is opened at the Fermi level. The distribution of Al and Si-based states in the valence and conduction band of AlSi corresponds well to that of Zn and Sb-based ones in ZnSb. Al_6Si_5 is a semiconductor: The Fermi level is located at a band gap with a size of about 0.7 eV (Figure 5b). This system has 38 electrons per formula unit, one more than Zn_6Sb_5. Thus, the proper composition of disordered β-Zn_4Sb_3, that is, $Zn_{13}Sb_{10}$ with 76 = 38×2 electrons per formula unit, ensures complete filling of the valence band, in agreement with the physical properties. Conversely, the 13–10 framework is a semiconductor for the Zn–Sb system but not for the Al–Si system.

This investigation reveals that the electronic structures of the high-coordination number frameworks found in zinc antimonides basically follow a rigid band behaviour. This is an important result. The kind of constituting s–p elements determines if a real band gap is opened at the Fermi level, or just a pseudogap expressed. However, the location of this

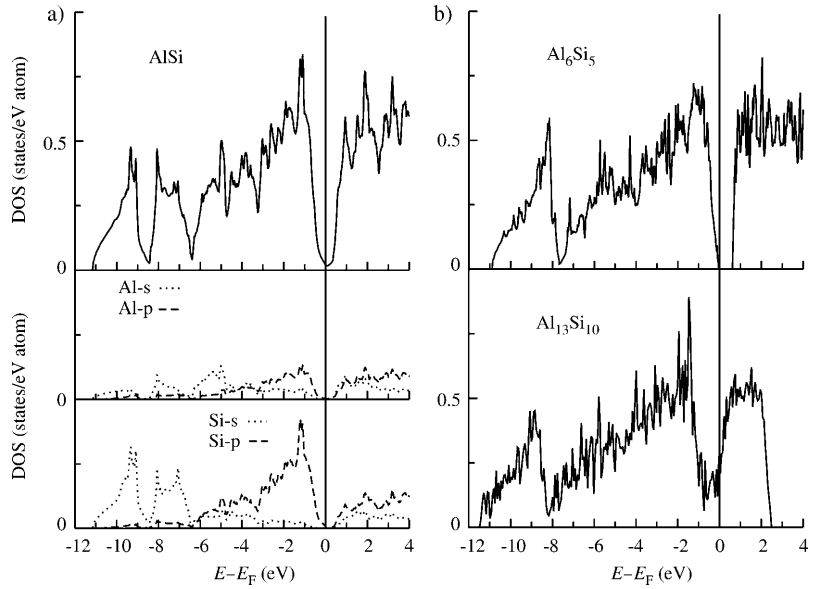

Figure 5. a) Electronic density of states (DOS) for AlSi. Top: total DOS, bottom: site and orbital decomposed DOS. b) DOS for Al_6Si_5 and $Al_{13}Si_{10}$. The distribution of the site and orbital decomposed components is very similar to AlSi and not shown. The Fermi level is indicated by a vertical line.

feature in the DOS and the shape of the DOS around the Fermi level are not dependent on the elemental combination. Finally, we mention that mixtures of Group 13 and 14 elements typically do not yield stable compounds. Figure 6 shows the formation energies for the hypothetical 1–1, 6–5, and 13–10 Al/Si frameworks with all values clearly positive. Most stable is Al_6Si_5, that is, the 6–5 framework displaying a real band gap. This band gap indicates that Al_6Si_5 could be an accessible, although metastable material. Interestingly, there are a number of metastable phases reported for the Al/Ge system.[26] Amongst them is Al_6Ge_5, which was assigned the rhombohedral structure of the 6–5 framework.[27] The calculated energy of formation for Al_6Ge_5 is 0.026 eVatom^{-1} and thus is considerably lower than that of Al_6Si_5.

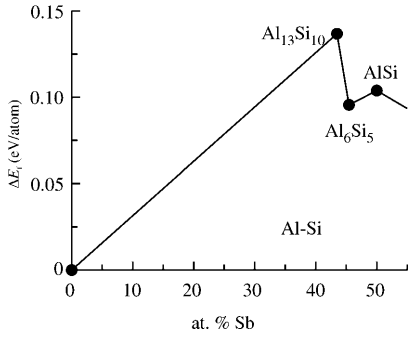

Figure 6. Energy of formation for AlSi, Al_6Si_5, and $Al_{13}Si_{10}$.

As a last step of our work we attempt to establish a bonding model for the 1–1 and 6–5 frameworks. We recall their peculiarity: The frameworks are s–p bonded and display a narrow band gap while at the same time the constituting atoms have coordination numbers larger than 4. Importantly, it is not immediately obvious to consider the structures of zinc antimonides as frameworks. Earlier efforts to rationalise the electronic structure of these compounds were performed on the basis of the Zintl–Klemm concept.[10–12] This implies an ionic (or at least polar) description of the structures. Zn would formally reduce Sb, which then forms an electron-precise polyanion on the basis of the $(8-N)$ valence rule. Interestingly, at first sight this description would apply: The formulas ZnSb = $(Zn^{2+})_2$ Sb_2^{4-} and $Zn_{13}Sb_{10}$ = $(Zn^{2+})_{13}(Sb1^{3-})_6(Sb2_2^{4-})_2$ account for the presence of short Sb–Sb distances characteristic of a single bond and isolated, that is, exclusively Zn coordinated, Sb atoms. However, the short Zn–Zn distances also present in the structures provide a problem. They are indicative of Zn–Zn interactions and not compatible with distances between Zn cations. Further, good thermoelectric materials have typically a low polarity—and a low polarity for zinc antimonides is suggested form our electronic structure analysis above, which reveals a rather high contribution of Zn based states to the valence band. Also, the fact that the peculiar electronic structures of Zn/Sb systems can be modelled by Al/Si systems is a strong argument for a framework description of zinc antimonide structures.

In order to achieve a bonding model for the 1–1 and 6–5 framework structures we take a look again at the local coordination of the constituting atoms. From Figures 1a and 2a we recognise a pattern for the coordination environments in zinc antimonides: Zinc atoms appear to be preferably five-coordinated and part of Zn_2Sb_2 diamonds. The coordination to the unlike neighbours is a distorted tetrahedral one. Sb atoms are tetrahedrally surrounded by either isolated Zn atoms or pairs of Zn atoms being part of diamonds. Thus, although higher coordination numbers than four are realised, coordination is ruled by an underlying tetrahedral principle. This fact tempts to firstly assign each atom in the framework a basis set of four sp^3 hybrid orbitals. In the next step, bonds not involved in diamonds are considered as two-centre two-electron (2c2e) bonds. (Note, that these bonds are shorter than the distances within diamonds, compare Figures 1a, 2a.) This leaves six basis functions for diamond ring bonding. It is important to note that this assignment holds for both types of frameworks: Zn-type atoms always participate with two basis functions and Sb-type atoms with one basis function to bonding in one particular diamond ring. (In

Zn_6Sb_5 Sb1 atoms are involved in two rings without changing this picture.) Now it is easy to assemble appropriate molecular orbitals (MOs) for the diamond ring (point group symmetry D_{2h}), which is shown in Figure 7. There are two

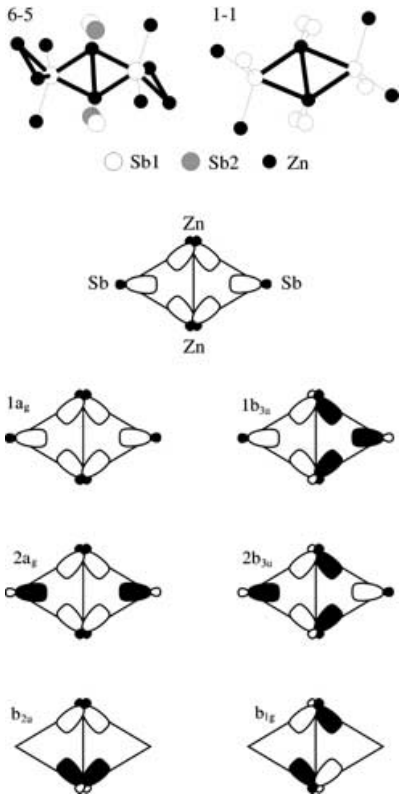

Figure 7. Four-centre four-electron (4c4e) bonding in the Zn_2Sb_2 diamond ring (D_{2h}). The top row figures show the tetrahedral-like coordination environments of the constituting atoms in the 1–1 and 6–5 frameworks. Bonds not involved in diamonds are considered as terminal 2c2e bonds. Then, Sb-type atoms donate one and Zn-type atoms two basis functions to ring bonding. Six molecular orbitals can be constructed of which two are bonding ($1a_g$ and $1b_{3u}$).

strongly bonding MOs ($1a_g$ and $1b_{3u}$), two slightly antibonding (b_{2u} and b_{1g}), and two strongly antibonding ones ($2a_g$ and $2b_{3u}$). With four electrons occupying the bonding MOs the diamond ring emerges as 4c4e bonded and an electron precise situation is attained corresponding to all states filled up to the narrow band gap. In particular, the diamond ring requires 10 electrons for 2c2e terminal bonding (three bonds and two bonds from the atoms defining the long and short diagonal, respectively) and four electrons for ring bonding. This is the situation of the 1–1 framework, which is electron precise for an electron count of 3.5 e^- per atom (i.e., ZnSb and AlSi). In the 6–5 framework diamonds are condensed to chains via the long diagonal. A chain can be expressed as $[S_2L_{2/2}]$ when denoting atoms at the short and long diagonal as S and L, respectively. Upon condensation ring bonding remains unaffected but L-type atoms loose one terminal bond. Thus, a chain requires six electrons for 2c2e terminal bonding and four electrons for ring bonding per unit $[S_2L_{2/2}]$, that is, per three atoms, and is electron precise for an electron count of 3.333 e^- per atom. The 6–5 framework consists of three chains making up the channel structure and additional tetrahedrally coordinated atoms T stuffing the channels (Sb2 atoms in Zn_6Sb_5). T-type atoms are only involved in 2c2e bonding, which requires four electrons. One bond is to another T atom and three bonds (to S) terminate diamond-ring chains. The 6–5 framework can be rewritten as $[S_2L_{2/2}]_3T_2$ and, thus, is electron precise for an electron count of 3.454 e^- per atom (i.e., Al_6Si_5).

The framework description of their structures puts zinc antimonides close to III/V semiconductors (GaAs, InSb) with the ZnS structure. The latter exhibit exclusively 2c2e bonding, whereas the more electron poor Zn/Sb frameworks develop localised multicentre bonding accompanied with a much higher structural complexity. The presented bonding model for the 1–1 and 6–5 frameworks is primarily a means of rationalising electron count in such electron poor, hypovalent, arrangements. The applied sp^3 hybrid basis functions are not necessarily justified from the band structures—especially not for zinc antimonides, where the Sb-s band is separated from the valence band. However, the same situation is encountered for tetrahedral III/V antimonides without questioning the 2c2e bonding picture. If further elaborating on our bonding model it would be natural to proceed from the 1–1 framework (separated diamonds) and 6–5 framework (one-dimensional chains of diamonds) to even more electron poor frameworks by further condensing diamonds via the long diagonal nodes (L atoms) into two- or three-dimensional assemblies. The recipe is simple; a terminal bond of an L atom is replaced by an additional diamond. A maximum number of four diamonds could be condensed at one node without changing the bonding picture. Such scenarios occur partly in the 13–10 framework and most likely also in the Zn_3Sb_2 structures. However, the bonding analysis of these more electron poor frameworks is obstructed by the fact that the sharp separation between nearest and next nearest neighbours present in the 1–1 and 6–5 frameworks is considerably weakened.

We conclude our electronic structure investigation by mentioning a recent article of Balakrishnarajan and Hoffmann who performed a detailed bonding analysis of a variety of molecular and extended boron structures containing a rhomboid (diamond) ring.[28] This work also dealt with the structure of β-SiB_3.[29] In β-SiB_3 = Si_4B_{12} an array of B_{12} icosahedra is interwoven with one-dimensional zigzag chains of Si_4 diamonds. Interestingly, these chains can be considered as fragments of the 1–1 framework. Each Si_4 diamond has 10 terminal bonds to either neighbouring diamonds or boron icosahedra. Thus, the zigzag chain is electron precise for an electron count of 3.5 e^- per atom. Since also all the boron atoms in the icosahedra attain a terminal bond the formula $Si_4^{2+}B_{12}^{2-}$ expresses an electron precise situation for each substructure in β-SiB_3. The Si_4^{2+} diamonds have not been recognised as 4c4e bonded entities in reference [26] and the example of β-SiB_3 demonstrates nicely the wider applicability of our bonding model.

Conclusion

The binary Zn/Sb system affords phases with complex crystal structures. These structures challenge crystallography because of the presence of disorder or incommensurate modulations—features, which in turn also influence the exact composition of the underlying phases. Only recently the structures of α and β-Zn_4Sb_3 and that of the high-temperature form of Zn_3Sb_2 could be established unambiguously. The actual composition of the Zn_4Sb_3 phases is $Zn_{13}Sb_{10}$. The structures of several more phases still await solution. ZnSb and Zn_4Sb_3 are narrow-gap semiconductors and display interesting thermoelectric properties. This is especially the case for disordered β-Zn_4Sb_3. We have analysed phase stability, electronic structure and bonding of ZnSb and Zn_4Sb_3 by means of first principles calculations. For Zn_4Sb_3 we find a peculiar situation: α-Zn_4Sb_3 is metastable and thermodynamic stability of β-Zn_4Sb_3 can only be explained when its structural disorder accounts for a large entropy contribution to free energy. The electronic density of states of the ZnSb and Zn_4Sb_3 ($Zn_{13}Sb_{10}$) phases reveal a band gap of 0.2–0.3 eV at the Fermi level, which is in agreement with measured transport properties. Importantly, we find that the electronic structure of zinc antimonides correspond to that of heteroatomic framework structures with a modest polarity. This is analogous to III/V semiconductors, but Zn/Sb frameworks are more electron poor and thus multicentre bonded. Interestingly, multicentre bonding appears localised and is confined to 4c4e bonded Zn_2Sb_2 diamond rings. These rings occur separated (in ZnSb) or condensed into chains (in Zn_4Sb_3) and are linked by classical 2c2b bonds. The peculiar electronic structure of Zn/Sb frameworks can also be modelled by Al/Si or Al/Ge systems, which proves their s–p bonded nature.

Another result of our study is the establishment of a clear relationship between disordered β-Zn_4Sb_3 and ordered low-temperature α-Zn_4Sb_3 by using nonclassically bonded Zn_2Sb_2 diamonds as structural building units. The structural description of α and β-Zn_4Sb_3 on the basis of diamond rings is superior to our previous attempt using nonbonded Zn_6 octahedra as a central structural unit[20] because it allows to identify explicitly the vacancies and interstitials of β-Zn_4Sb_3 in the structure of α-Zn_4Sb_3. This is an important issue: The high thermoelectric performance of β-Zn_4Sb_3 originates in its exceptional low thermal conductivity, which is intimately connected to the structural disorder. At the moment the nature of the disorder in β-Zn_4Sb_3 is not clear. Cargoni et al. proposed static disorder while modelling β-Zn_4Sb_3 as a mixture of unit cells with different concentrations of vacancies and interstitials.[12] However, the disorder could as well be dynamic with rapidly exchanging vacancies and interstitials. Currently we are working on the elucidation of the puzzling α–β order–disorder transition, which should provide an answer to this question. The final goal is a complete understanding of the remarkable thermoelectric properties of Zn_4Sb_3. Such an understanding must also provide some general additional insight into the mechanism of thermal conductivity, which is the most involved contribution to thermoelectric efficiency, and thus guide the search for improved materials.

Computational Details

Total energy calculations for Zn/Sb and hypothetical Al/Si compounds were performed with the frozen core all-electron Projected Augmented Wave (PAW) method,[30] as implemented in the program VASP.[31] The orthorhombic structure of ZnSb (1–1 framework), the idealised rhombohedral structure of β-Zn_4Sb_3 (6–5 framework) and the triclinic structure of α-Zn_4Sb_3 structure (13–10 framework) were considered. As structural input the crystallographic data according to references [6,20,22] were used. The cut-off energy for the plane wave expansion was set to 350 eV. The cut-off for the augmentation charges was set to 550 eV. We used the same cut-off for all structures in order to extract accurate formation energies. Exchange and correlation effects were treated with the generalized gradient approximation (GGA).[32] The integration over the Brillouin zone (BZ) was done on a grid of special k points determined according to the Monkhorst–Pack scheme,[33] by using varying grids depending on the unit cell. For the triclinic 13–10 frameworks we applied a $4\times4\times4$ k points grid. For the 1–1 and 6–5 frameworks $8\times8\times8$ k point grids and for the pure elements even finer grids of k points were used. The atomic position parameters and lattice parameters of all structures were relaxed for a set of constant volumes until forces had converged to at least 0.01 eV Å^{-1}. The relaxation procedure was carried out according to the Methfessel–Paxton scheme,[34] while accurate total energy calculations were done with the linear tetrahedron method with Blöchl corrections.[35] All necessary convergence tests were performed and total energies were converged to within 0.1 meVatom^{-1}.

Acknowledgement

This work was supported by the Swedish Research Council (VR).

[1] a) J. D. Corbett, *Angew. Chem. Int. Ed.* **2000**, *39*, 670; b) J. D. Corbett, *Inorg. Chem.* **2000**, *39*, 5178.
[2] G. J. Miller, C.-S. Lee, W. Choe in *Inorganic Chemistry Highlights* (Eds.: G. Meyer, D. Naumann, L. Wesemann), Wiley-VCH, Weinheim, Germany, **2002**, p. 21.
[3] C. Lupu, C. Downie, A. M. Guloy, T. A. Albright, J.-G. Mao, *J. Am. Chem. Soc.* **2004**, *126*, 4386.
[4] T. S. Massalski, *Binary Alloy Phase* ed. *Diagrams*, 2nd American Society for Metals, Metals Park (OH) USA, **1990**.
[5] V. Izard, M. C. Record, J. C. Tedenac, S. G. Fries, *CALPHAD* **2001**, *25*, 567.
[6] K. E. Almin, *Acta Chem. Scand.* **1948**, *2*, 400.
[7] Y. A. Ugai, T. A. Marshakova, V. Y. Shevchenko, N. P. Demina, *Izv. Akad. Nauk SSSR, Neorg. Mater.* **1969**, *5*, 1381.
[8] V. Y. Shevchenko, V. A. Skripkin, Y. A. Ugai, T. A. Marshakova, *Izv. Akad. Nauk. SSSR, Neorg. Mater.* **1968**, *4*, 1359.
[9] T. Souma, G. Nakamoto, M. Kurisu, *J. Alloys Compd.* **2002**, *340*, 275.
[10] Y. Mosharivskyj, A. O. Pecharsky, S. Bud'ko, G. J. Miller, *Chem. Mater.* **2004**, *16*, 1580.
[11] G. J. Snyder, M. Christensen, E. Nishibori, T. Caillat, B. B. Iversen, *Nat. Mater.* **2004**, *3*, 458.
[12] F. Caroni, E. Nishibori, P. Rabiller, L. Bertini, G. J. Snyder, M. Christensen, C. Gatti, B. B. Iversen, *Chem. Eur. J.* **2004**, *10*, 3861.
[13] M. Boström, S. Lidin, *J. Alloys Compd.* **2004**, *376*, 49.
[14] a) M. Telkes, *J. Appl. Phys.* **1954**, *25*, 765; b) *CRC Handbook of Thermoelectrics* (Ed.: D. M. Rowe), CRC Press, Florida, **1995**, p. 139.

[15] M. Tapiero, S. Tarabichi, J. G. Gies, C. Noguet, J. P. Zielinger, M. Joucla, J. L. Loison, M. Robino, J. Herion, *Sol. Energy Mater.* **1985**, *12*, 257.
[16] T. Caillat, J.-P. Fleurial, A. Borshchevsky, *J. Chem. Phys.* **1997**, *58*, 1119.
[17] F. J. DiSalvo, *Science* **1999**, *285*, 703.
[18] A. Bentien, B. B. Iversen, J. D. Bryan, G. D. Stucky, A. E. C. Palmqvist, A. J. Schultz, R. W. Henning, *J. Appl. Phys.* **2002**, *91*, 5694.
[19] M. Christensen, B. B. Iversen, L. Bertini, C. Gatti, M. Toprak, M. Muhammed, E. Nishibori, *J. Appl. Phys.* **2004**, *96*, 3148.
[20] J. Nylén, M. Andersson, S. Lidin, U. Häussermann, *J. Am. Chem. Soc.* **2004**, *126*, 16306.
[21] β-Zn_4Sb_3 is obtained from stoichiometric mixtures of Zn and Sb, which are heated to 870–920 K and subsequently subjected to different cooling or quenching procedures (see refs. [5, 9, 10, 11, 20, 22]).
[22] H. W. Mayer, I. Mikhail, K. Schubert, *J. Less-Common Met.* **1978**, *59*, 43.
[23] The CIF may be obtained as supporting information accompanying ref. [20] or from Fachinformationszentrum Karlsruhe, crysdata@fiz-karlsruhe.de, on quoting the depository number CSD-413936.
[24] Good thermoelectric performers are typically semiconductors with a sufficiently low resistivity ρ, that is, heavily doped. Metals have a desirable low ρ, but also low thermopowers S and high thermal conductivities κ due to a large electronic contribution. In general, as S increases, so does ρ. Materials with large band gaps usually possess large lattice thermal conductivity.
[25] G. A. Slack in *CRC Handbook of Thermoelectrics* (Ed.: D. M. Rowe), CRC Press Inc., Florida, **1995**, p. 407.
[26] M. J. Kaufman, H. L. Fraser, *Acta Metallogr.* **1985**, *33*, 191.
[27] R. Vincent, D. R. Exelby, *Acta Crystallogr. Sect. A* **1995**, *51*, 801.
[28] M. M. Balakrishnarajan, R. Hoffmann, *J. Am. Chem. Soc.* **2004**, *126*, 13119.
[29] J. R. Salvador, D. Bilc, S. D. Mahanti, M. G. Kanatzidis, *Angew. Chem.* **2003**, *115*, 1973; *Angew. Chem. Int. Ed.* **2003**, *42*, 1929.
[30] a) P. E. Blöchl, *Phys. Rev. B* **1994**, *50*, 17953; b) G. Kresse, J. Joubert, *Phys. Rev. B* **1999**, *59*, 1758.
[31] a) G. Kresse, J. Hafner, *Phys. Rev. B* **1993**, *48*, 13115; b) G. Kresse, J. Furthmüller, *Comput. Mater. Sci.* **1996**, *6*, 15.
[32] a) Y. Wang, J. P. Perdew, *Phys. Rev. B* **1991**, *44*, 13298; b) J. P. Perdew, J. A. Chevary, S. H. Vosko, K. A. Jackson, M. R. Pederson, D. J. Singh, C. Fiolhais, *Phys. Rev. B* **1992**, *46*, 6671.
[33] H. J. Monkhorst, J. D. Pack, *Phys. Rev. B* **1972**, *13*, 5188.
[34] M. Methfessel, A. T. Paxton, *Phys. Rev. B* **1989**, *40*, 3616.
[35] O. Jepsen, O. K. Andersen, *Solid State Commun.* **1971**, *9*, 1763.

Received: January 10, 2005
Published online: June 7, 2005